arXiv:1402.1991v2 [cond-mat.dis-nn] 4 Aug 2014

The Ising Spin Glass in dimension four; non-universality

P. H. Lundow[1] and I. A. Campbell[2]

[1]*Department of Mathematics and Mathematical Statistics, Umeå University, SE-901 87, Sweden*
[2]*Laboratoire Charles Coulomb, Université Montpellier II, 34095 Montpellier, France*

Extensive simulations are made on Ising Spin Glasses (ISG) with Gaussian, Laplacian and bimodal interaction distributions in dimension four. Standard finite size scaling analyses near and at criticality provide estimates of the critical inverse temperatures β_c, critical exponents, and critical values of a number of dimensionless parameters. Independent estimates are obtained for β_c and the exponent ν from thermodynamic derivative peak data. A detailed explanation is given of scaling in the thermodynamic limit with the ISG scaling variable $\tau = 1-\beta^2/\beta_c^2$ and the appropriate scaling expressions. Data over the entire paramagnetic range of temperatures are analysed in order to obtain further estimates of the critical exponents together with correction to scaling terms. The Privman-Fisher ansatz then leads to compact scaling expressions for the whole paramagnetic regime and for all sample sizes L. Comparisons between the 4d ISG models show that the critical dimensionless parameters characteristic of a universality class, and the susceptibility and correlation length critical exponents γ and ν, depend on the form of the interaction distribution. From these observations it can be deduced that critical exponents are not universal in ISGs, at least in dimension four.

PACS numbers: 75.50.Lk, 05.50.+q, 64.60.Cn, 75.40.Cx

INTRODUCTION

The universality of critical exponents is an important and remarkably elegant property of standard second order transitions, which has been explored in great detail through the Renormalization Group Theory (RGT). The universality hypothesis states that for all systems within a universality class the critical exponents are rigorously identical and do not depend on the microscopic parameters of the model. However, universality is not strictly universal; there are known "eccentric"models which are exceptions and violate the universality rule in the sense that their critical exponents vary continuously as functions of a control variable. The most famous example is the eight vertex model solved exactly by Baxter [1]. The exceptional physical conditions which apply in this case were discussed in detail in Ref. [2].

For Ising Spin Glasses (ISGs), the form of the interaction distribution is a microscopic control parameter. It has been assumed tacitly or explicitly that the members of the ISG family of transitions obey standard universality rules, following the generally accepted statement that "Empirically, one finds that all systems in nature belong to one of a comparatively small number of universality classes"[3]. One should underline the word "empirically"; we know of no formal proof that universality must hold in ISGs. It was found thirty years ago that the ϵ-expansion for the critical exponents [4] in ISGs is not predictive since the first few orders have a non-convergent behavior and higher orders are not known. This can be taken as an indication that a fundamentally different theoretical approach is required for RGT at spin glass transitions. Indeed "classical tools of RGT analysis are not suitable for spin glasses" [5–7], although no explicit theoretical predictions have been made so far concerning universality.

ISG transition simulations are much more demanding numerically than are those on, say, pure ferromagnet transitions with no interaction disorder. The traditional approach in ISGs has been to study the temperature and size dependence of observables in the near-transition region and to estimate the critical temperature and exponents through finite size scaling (FSS) relations after taking means over large numbers of samples. Finite size corrections to scaling must be allowed for explicitly which can be delicate. From numerical data, claims of universality have been made repeatedly for ISGs [10–12, 14] even though the estimates of the critical exponents have varied considerably over the years (see Ref. [11] for a tabulation of historic estimates).

On this FSS approach the critical inverse temperature β_c estimates are very important for deducing reliable values for the critical exponents [16]. Here we also obtain independent estimates for β_c and for the exponent ν through the thermodynamic derivative peak (pseudocritical temperature) technique. The estimates for β_c and for ν from this analysis can be considered to be independent of each other and the correction to scaling only plays a minor role. With the best estimates for β_c in hand the numerical data in the thermodynamic limit (ThL) regime are then analysed with the scaling variable $\tau = (1-\beta^2/\beta_c^2)$ appropriate to ISGs, together with scaling expressions which cover the entire paramagnetic temperature regime rather than being limited to the narrow critical region [17]. Once values for all critical parameters have been obtained by combining information from FSS, pseudocritical temperature, and ThL data, through the Privman-Fisher ansatz [18] compact scaling expressions can be obtained covering the entire paramagnetic temperature range and all sizes L.

From a comparison of the critical values for dimensionless parameters and for the critical exponent values, each of which is characteristic of a universality class, we conclude that the Gaussian, Laplacian and bimodal ISGs in dimension four are not in the same universality class. This counter example to the general rule implies that universality does not hold in ISGs. It is relevant that it has already been shown experimentally that in Heisenberg spin glasses the critical exponents depend on the strength of the Dzyaloshinski-Moriya interaction [19].

ISING SPIN GLASS SIMULATIONS

The Hamiltonian is as usual

$$\mathcal{H} = -\sum_{ij} J_{ij} S_i S_j \tag{1}$$

with the near neighbor symmetric distributions normalized to $\langle J_{ij}^2 \rangle = 1$. The Ising spins live on simple hypercubic lattices with periodic boundary conditions. We have studied the bimodal (J4d) model with a $\pm J$ interaction distribution, Gaussian (G4d) model with a $\exp(-J^2)$ interaction distribution, and Laplacian (L4d) model with a $\exp(-|J|)$ interaction distribution, all in dimension 4. We will compare with published measurements on 4d ISGs.

The simulations were carried out using the exchange Monte-Carlo method for equilibration using so called multi-spin coding, on 2^{14} (up to $L = 7$) or 2^{13} for larger L individual samples at each size. An exchange was attempted after every sweep with a success rate of at least 30%. At least 40 temperatures were used forming a geometric progression reaching down to $\beta_{\max} = 0.55$ for J4d, $\beta_{\max} = 0.58$ for G4d and $\beta_{\max} = 0.65$ for L4d. This ensures that our data span the critical temperature region which is essential for the FSS fits. Near the critical temperature the β step length was at most 0.004. The various systems were deemed to have reached equilibrium when the sample average susceptibility for the lowest temperature showed no trend between runs. For example, for $L = 12$ this means about 200000 sweep-exchange steps.

After equilibration, at least 200000 measurements were made for each sample for all sizes, taking place after every sweep-exchange step. Data were registered for the energy $E(\beta, L)$, the correlation length $\xi(\beta, L)$, for the spin overlap moments $\langle |q| \rangle$, $\langle q^2 \rangle$, $\langle |q|^3 \rangle$, $\langle q^4 \rangle$ and the corresponding link overlap q_ℓ moments. In addition the correlations $\langle E(\beta, L), U(\beta, L) \rangle$ between the energy and observables $U(\beta, L)$ were also registered so that thermodynamic derivatives could be evaluated using the relation $\partial U(\beta, L)/\partial\beta = \langle U(\beta, L), E(\beta, L) \rangle - \langle U(\beta, L) \rangle \langle E(\beta, L) \rangle$ where $E(\beta, L)$ is the energy [28]. Bootstrap analyses of the errors in the derivatives as well as in the observables $U(\beta, L)$ themselves were carried out.

FINITE SIZE SCALING

For the present analysis we have first observed the FSS behavior of various dimensionless parameters, not only the familiar Binder cumulant

$$g(\beta, L) = \frac{1}{2}\left(3 - \frac{[\langle q^4 \rangle]}{[\langle q^2 \rangle])^2}\right) \tag{2}$$

and the correlation length ratio $\xi(\beta, L)/L$, but also other observables showing analogous critical behavior. One alternative dimensionless parameter

$$W = \frac{1}{\pi - 2}\left(\pi \frac{\langle |m| \rangle^2}{\langle m^2 \rangle} - 2\right) \tag{3}$$

was introduced in the Ising ferromagnet context in [33]. In the ISGs m can be replaced by q so

$$W_q = \frac{1}{\pi - 2}\left(\pi \frac{[\langle |q| \rangle]^2}{[\langle q^2 \rangle]} - 2\right) \tag{4}$$

In the same spirit we have also introduced the dimensionless parameter

$$h(\beta, L) = \frac{1}{\sqrt{\pi} - \sqrt{8}}\left(\sqrt{\pi} \frac{[\langle |q^3| \rangle]}{[\langle q^2 \rangle]^{3/2}} - \sqrt{8}\right) \tag{5}$$

We have also registered the non-self averaging parameter U_{22}, the kurtosis of the spin overlap distribution, and the moments of the absolute spin overlap distribution, together with the variance and kurtosis of the link overlap distribution [34, 35]. Only a fraction of these data are reported here.

Analyses with the traditional technique of estimating crossing point temperatures $[\beta_{\rm cross}, L]$, defined through $U(\beta_{\rm cross}, L) = U(\beta_{\rm cross}, 2L)$, have disadvantages. The statistical errors in both sizes L and $2L$ contribute to the uncertainty of the crossing temperature; the scaling correction to the smaller size L dominates and is combined with the numerical difficulty in equilibrating at the larger size $2L$. Instead we interpolate using the data points for each $U(\beta, L)$ so as to obtain sets of data $U(\beta_f, L)$ for a few fixed β_f in the critical region, after making a first rough estimate of β_c. (It is important to span the range of temperatures on both sides of the true β_c). We then make a global fit with the standard FSS expression, valid in the critical region if there is a single dominant scaling correction term :

$$U(\beta, L) = U(\beta_c, \infty) + AL^{-\omega} + B(\beta - \beta_c)L^{1/\nu} \tag{6}$$

The fit uses all the FSS region data, and gives output estimates, with error bars, for β_c and the critical exponents ν and ω. The parameters of Eq. (6), and their error bars at the 95% level, were found by using Mathematica's built-in routines for nonlinear model fitting. The data points for each U were obtained at some 20 fixed

β_f near β_c ($0.98 < \beta_f/\beta c < 1.02$), using cubic spline interpolation. Thus the six parameters are based on some 200-300 data points from different β and L. The quality of the fit is checked by looking at not only the adjusted R-square index, which is always extremely close to 1 in our fits. A better test is to see whether the distribution of deviations between data and fitted model, so called standardized residuals, can be considered zero by using Mathematica's built-in zero-location tests, using the sign-test or T-test. The fitted models reported here pass these tests at the 5% level.

THERMODYNAMIC DERIVATIVE PEAKS ANALYSIS

The thermodynamic derivative (pseudocritical temperature) analysis can be an efficient method for analyzing data in a ferromagnet or an ISG. Near criticality in a ferromagnet for many observables U the heights of the peaks $D_{\max}(U, L)$ of the thermodynamic derivatives $D(U, L) = \partial U(\beta, L)/\partial\beta$ scale for large L as [28, 29]

$$\max\left[\frac{\partial U(\beta, L)}{\partial \beta}\right] \propto L^{1/\nu}\left(1 + aL^{-\omega/\nu}\right) \qquad (7)$$

A peak height $D_{\max}(U, L)$ against L log-log plot tends linearly to $1/\nu$ at large L and so provides an estimate for ν directly without the need for a value of β_c as input. Corrections to scaling only play a minor role.

The temperature location of the derivative peak $\beta_{\max}(U, L)$ also scales as

$$\beta_c - \beta_{\max}(L) \propto L^{-1/\nu}(1 + bL^{-\omega/\nu}) \qquad (8)$$

so as both $\beta_c - \beta_{\max}(L)$ and $\max[\partial U(\beta, L)/\partial\beta]$ vary as $L^{-1/\nu}$ at large L, a plot of the peak locations against the inverse peak heights tends linearly to β_c at large L. This estimate is independent of the FSS estimate.

The observables used for $U(\beta, L)$ [28] can be for instance the Binder cumulant $g(\beta, L)$, the logarithm of the finite size susceptibility $\ln\chi(\beta, L)$, or the logarithm of the absolute value of the magnetisation $\ln(|m|(\beta, L))$. Each of these data sets can give independent estimates of ν and β_c without any initial knowledge of either parameter. For a ferromagnet, Ferrenberg and Landau [28] find this form of analysis significantly more accurate than the standard Binder cumulant crossing approach.

All plots of this type with different observables U should extrapolate consistently to the true β_c, with the confluent correction only appearing as a small L modification to the straight line. Provided that the peaks for the chosen observable fall reasonably close to β_c, these data are in principle much simpler to analyse than those from the Binder crossing technique where one must estimate simultaneously β_c and ν together with the strength a and the exponent ω of the leading correction term. For ISGs very much the same thermodynamic differential peak methodology can be used as in the ferromagnet. As far as we are aware this analysis has not been used previously in the ISG context.

THERMODYNAMIC LIMIT SCALING VARIABLES AND EXPRESSIONS

We will give a detailed discussion of scaling in ferromagnets and in ISGs in the thermodynamic limit (ThL) regime, using the scaling variable $\tau = 1 - \beta/\beta_c$ in ferromagnets and $\tau = 1 - \beta^2/\beta_c^2$ in ISGs [17], as this approach has been widely misunderstood or simply ignored.

The ThL regime concerns all the data for each L which obey the condition $L \gg \xi(\beta, \infty)$ where $\xi(\beta, \infty)$ is the infinite sample size correlation length for inverse temperature β. In this regime all observables are independent of L and so are equal to their infinite size values as measured for instance by long series HTSE sums. A rule of thumb for this regime is $L/\xi(\beta, \infty) \gtrsim 6$. In order to estimate critical exponents, an extrapolation to criticality at β_c must complete the overall fit to ThL data taken at finite L.

In the literature, numerical data on critical transition phenomena are almost always analysed using $t = 1 - T/T_c$ as the scaling variable, following the standard critical regime prescription of the Renormalization Group Theory (RGT). In particular t scaling has been used in recent ISG studies [12, 13, 20]. However with this variable, explicit analyses of numerical data are limited to the finite size scaling $L/\xi(\beta, \infty) \ll 1$ regime within a narrow critical region in temperature; t diverges at infinite temperature, so when t is used outside the critical temperature region, corrections to scaling inevitably proliferate.

In ferromagnets, for well over fifty years the scaling variable $\tau = 1 - \beta/\beta_c$ has been used for the analysis of the high temperature scaling expansion (HTSE) for the susceptibility; in particular the scaling variable τ was used in the original discussion of confluent corrections to scaling in ferromagnets by Wegner [21] which led to the important ThL susceptibility expression

$$\chi(\beta, \infty) = C_\chi \tau^{-\gamma}\left(1 + a_\chi \tau^\theta + b_\chi \tau + \cdots\right) \qquad (9)$$

The first correction term is the confluent correction and the second an analytic correction.

In the critical region τ and t become equivalent, but as $\tau \to 1$ at infinite temperature (where $\chi(\beta) \to 1$) instead of diverging, the τ expression is well controlled over the whole paramagnetic regime. In principle there can be many correction terms in Eq. (9) but in practice to high precision a leading term and one single further effective correction term are generally sufficient for an analysis at the level of precision of numerical data. This is because the leading terms in the HTSE provide strict closure conditions on the Eq. (9) series. Thus for the

canonical Ising ferromagnet in dimension two, there are five or more further well identified correction terms [8] but in practice with one single weak effective correction term beyond the leading term, the expression Eq. (9) represents the temperature dependence of the ThL susceptibility to high precision from criticality to infinite temperature [22]. The same remark holds for Ising ferromagnets in dimension three [23, 24]. In ferromagnets the use of t as the scaling variable leads to a "crossover"to a high temperature mean field behavior [25], which is a pure artefact [24]. Note that for ferromagnets with zero temperature ordering $\tau = 1 - \tanh\beta$ can be a suitable variable [9].

Following a protocol well-established in ferromagnets [26, 27] one can define a temperature dependent effective exponent for the susceptibility

$$\gamma(\tau) = -\frac{\partial \ln \chi(\tau)}{\partial \ln \tau} \tag{10}$$

$\gamma(\tau)$ tends to the critical γ as $\beta \to \beta_c$, and to exactly $z\beta_c$ as $\beta \to 0$, where z is the number of nearest neighbors so $2d$ in simple [hyper]-cubic lattices.

For the ThL regime $\gamma(\tau)$ can be written

$$\gamma(\tau) = \gamma - \frac{a_\chi \theta \tau^\theta + b_\chi y \tau^y}{1 + a_\chi \tau^\theta + b_\chi \tau^y} \tag{11}$$

including the leading order confluent scaling term and a further effective higher order correction term. The exact infinite temperature $\tau = 1$ HTSE condition on the fit parameters is

$$\gamma - \frac{a_\chi \theta + b_\chi y}{1 + a_\chi + b_\chi} = 2d\beta_c \tag{12}$$

The estimates for the critical γ and θ should be consistent with those from FSS and from pseudocritical peak temperature analyses.

Again in Ising ferromagnets, the analogous ThL expression for the second moment correlation length $\xi(\tau)$ is [17]

$$\xi(\tau) = C_\xi \beta^{1/2} \tau^{-\nu} \left(1 + a_\xi \tau^\theta + \cdots\right) \tag{13}$$

The factor $\beta^{1/2}$ arises because the generic infinite temperature limit behavior is $\xi(\tau)/\beta^{1/2} \to 1$. The temperature dependent effective exponent is then

$$\nu(\tau) = -\frac{\partial \ln(\xi(\tau)/\beta^{1/2})}{\partial \ln \tau} \tag{14}$$

so with a two correction term relation:

$$\nu(\tau) = \nu - \frac{a_\xi \theta \tau^\theta + b_\xi y \tau^y}{1 + a_\xi \tau^\theta + b_{xi} \tau^y} \tag{15}$$

$\nu(\tau)$ tends to the critical ν as $\beta \to \beta_c$, and to $d\beta_c$ as $\beta \to 0$ for ferromagnets on simple [hyper]-cubic lattices.

Another effective exponent for ferromagnets is $2 - \eta(\beta) = \partial \ln(\chi(\beta, L))/\partial \ln(\xi(\beta, L)/\beta^{1/2})$ which tends to the critical $2 - \eta(\beta_c)$ at the large L critical temperature limit. Plotted against $\beta^{1/2}/\xi(\beta, L)$ the plot of this exponent is defined numerically without reference to β_c (as against the plots of $\gamma(\tau)$ and $\nu(\tau)$). In the analogous ISG plots β is replaced by β^2 and $\beta^{1/2}$ by β, see Figs. 6, 13 and 20. The extrapolation giving the estimate for $2 - \eta(\beta_c^2$ is independent of the estimate for β_c.

In ISGs, because the effective interaction energy parameter is $\langle J^2 \rangle$ and not $\langle J \rangle$, the appropriate inverse "temperature"parameter is β^2 not β, so the appropriate scaling variable is $\tau = 1 - (\beta/\beta_c)^2$, (or $w = 1 - (\tanh(\beta)/\tanh(\beta_c))^2$ for the bimodal ISG case). This ISG scaling variable τ (or w) was used for the analysis of the ThL ISG susceptibility immediately after the introduction of the Edwards-Anderson ISG model [17, 30–32]. With this τ the ThL susceptibility relations Eqs. (9),(10) and (11) are formally the same as in the ferromagnet.

$$\chi(\tau) = C_\chi \tau^{-\gamma} \left(1 + a_\chi \tau^\theta + \cdots\right) \tag{16}$$

and $\gamma(\tau)$ tends to the critical γ as $\beta^2 \to \beta_c^2$. The exact high temperature limit from HTSE is $\gamma(\tau) \to 2d\beta_c^2$ as $\beta^2 \to 0$ in simple [hyper]-cubic lattices.

The appropriate ISG correlation length expression is

$$\xi(\tau) = C_\xi \beta \tau^{-\nu} \left(1 + a_\xi \tau^\theta + \cdots\right) \tag{17}$$

The factor β arises from the generic form of the ISG $\xi(\beta)$ high temperature series [17]. The temperature dependent ISG effective exponent is

$$\nu(\tau) = -\frac{\partial \ln(\xi(\beta)/\beta)}{\partial \ln \tau} \tag{18}$$

We know of no HTSE calculations of the second moment correlation length in ISGs which would lead to an exact $\beta \to 0$ limit for $\nu(\tau)$ in ISGs. As an empirical rule deduced from the χ HTSE analysis of Ref. [32], in simple hyper-cubic lattices of dimension d this limit is $\nu(\beta = 0) = (d - K/3)\beta_c^2$ where K is the kurtosis of the interaction distribution.

FSS analyses rely mainly on the size dependance of the critical behavior of observables $U(\beta_c, L)$ and their derivatives $[\partial U(\beta, L)/\partial\beta]_{\beta_c}$. For the dimensionless parameters such as the cumulant $U_4(\beta, L) = \langle m(\beta, L)^4 \rangle / \langle m(\beta, L)^2 \rangle^2$ or alternatively the Binder parameter $g(\beta, L) = (3 - U_4)/2$, and the correlation length ratio $\xi(\beta, L)/L$, the form of the critical size dependence

$$U(\beta_c, L) = U_{\beta_c,\infty} + K_U L^{1/\nu} \left(1 + a_U L^{-\omega} + \cdots\right) \tag{19}$$

and the critical derivative expression

$$\left[\frac{\partial U(\beta, L)}{\partial \beta}\right]_{\beta_c} = K_{U'} L^{1/\nu} \left(1 + a_{U'} L^{-\omega} + \cdots\right) \tag{20}$$

can be retained unaltered with τ scaling for very small $1 - \beta/\beta_c$ both for ferromagnets and for ISGs.

It has been pointed out on general grounds [11, 12] that the logarithmic derivative of the susceptibility has the form

$$\frac{\partial\chi(\beta,L)/\partial\beta}{\chi(\beta,L)} = K_\chi L^{1/\nu}\left(1 + a_\chi L^{-\omega} + \cdots\right) + K_1 \quad (21)$$

No evaluation was proposed for the constant term K_1 in Ref. [11, 12]. From the leading order τ scaling finite size expression for $\chi(\beta, L)$ [17] it is easy to show that $K_1 = -(2-\eta)/2\beta_c$ in a ferromagnet [23]. In an ISG the constant term in $(\partial\chi(\beta^2, L)/\partial\beta^2)/\chi(\beta^2, L)$ is $K_1 = -(2-\eta)/2\beta_c^2$. As pointed out in Ref. [11], for many years the published estimates of the exponent ν in ISGs were wrong by factors of the order of 2 because a constant K_1 term was not included in the FSS susceptibility analyses.

As stated above, the ThL regime is limited for each L by a condition for which a rule of thumb is $L/\xi(\beta,\infty) \gtrsim 6$, and an extrapolation to criticality must complete the overall fit to all the ThL data in order to estimate critical exponents. The accuracy of this extrapolation depends on a figure of merit, the minimum value of τ for which the ThL condition still holds for samples of size L. This figure of merit in ISGs can be taken to be

$$\tau_{\min} \sim (L/6\beta_c)^{-1/\nu} \quad (22)$$

In dimension 4 with $\beta_c \sim 0.5$ and $\nu \sim 1$ the condition implies $\tau_{\min} \sim 0.25$ if the largest size used is $L_m = 12$. This $\tau_{\min}$ corresponds to $\beta_{\min} \sim 0.9\beta_c$ so to a temperature within 10% of the critical temperature. It should be underlined that in dimension 3 with the appropriate parameters for ISGs, $\beta_c \sim 1$, $\nu \sim 2.5$, to reach $\tau_{\min} \sim 0.25$ would require sample sizes to $L_m \sim 200$, well beyond the maximum sizes which have been studied numerically so far in 3d ISGs. When fitting to obtain the extrapolation, no *a priori* assumption is made as to the value of the dominant scaling correction exponent, which can be that of the confluent correction (as in the 3d ferromagnet [23]), of an analytic correction (as in the 2d ferromagnet [22]), or of a high order effective correction if the prefactors of the low order terms happen to be very weak. The exponent values and the prefactor a_χ for the leading term are obtained from the fit. It can be noted that an exactly equivalent procedure is followed in the traditional fits to FSS data, where extrapolations are made from finite L to infinite size. The FSS correction exponent ω and the ThL correction exponent θ are related by $\omega = \theta/\nu$. This rule provides an important consistency test for FSS and ThL analyses on each system. The strength of the leading correction prefactor a is an important parameter for both FSS and ThL analyses, which is rarely quoted explicitly in publications on numerical work on ISGs.

OVERALL SCALING PLOT FOR ISING SPIN GLASSES

One method of showing ThL and derivative peak $\chi(\beta, L)$ data together in ISGs (following a suggestion by K. Hukushima) is to plot $y = \partial\beta^2/\partial\ln\chi(\beta, L)$ against $x = \beta^2$, see Figs. 1, 8 and 15. (One can also plot $y = \partial\beta^2/\partial\ln(\xi(\beta, L)/\beta)$ against $x = \beta^2$). These plots are purely displays of raw measured data and do not require β_c or any other parameter as input.

Each individual curve consists of data for a given L. Following the derivative peak discussion above, on this plot the set of minima points for large L extrapolate linearly to the critical point $x = \beta_c^2$ at $y = 0$.

The envelope curve corresponding to the data which for each L are in the ThL regime and its extrapolation to the critical point can be fitted by an expression :

$$\frac{\partial\beta^2}{\partial\ln\chi(\beta)} = \frac{(\beta^2 - \beta_c^2)(1 + a_\chi\tau^\theta)}{\gamma + (\gamma - \theta)a_\chi\tau^\theta} \quad (23)$$

A further correction term can be readily included if needed. The intercept $y = 0$ of the fit curve occurs at the critical point where $x = \beta_c$ and the initial slope starting at the intercept is $\partial y/\partial x = -1/\gamma$. The fit parameters are β_c, γ, θ and a_χ. The $\chi(\beta, L)$ fit must obey the condition that at $x = 0$, $y \equiv 1/2d$, so as β_c is known from the minima point and corrections beyond the leading one are negligible, there are just two free fit parameters. As a bonus, all the data used for the estimates come from temperatures above the critical temperature, where equilibration is easier to achieve than at and below criticality. Thus from an analysis of susceptibility derivative data alone, it is possible to estimate all the principal critical parameters $(\beta_c, \gamma, \nu, \theta)$ for each model.

ANALYTIC CORRECTIONS TO SCALING IN ISGS

It will be noted that the ThL data analyses presented here show no evidence for the presence of an analytic correction term proportional to τ, which if it exists should become dominant as criticality is approached when the confluent θ is greater than 1.

In a ferromagnet the leading analytic term is due to the field dependence of the analytic part of the free energy. We know of no *a priori* estimate of the strength of such terms in the ISG context, but it is plausible that they are intrinsically weak because the field is only present at higher order. HTSE analyses, particularly the M1 and M2 techniques [32], should be sensitive to the presence of analytic terms. In the HTSE measurements of Klein *et al.* [31] an explicit test was made for an analytic correction in the 4d bimodal ISG. No evidence was found for such a term. In all the more extensive HTSE analy-

ses of Ref. [32] the leading ThL correction term effective exponent θ was always significantly greater than 1.

It can be noted that for dimensional reasons, FSS corrections $L^{-\omega_i}$ have exponents related to the equivalent ThL exponents through $\omega_i = \theta_i/\nu$. So for ISGs in dimension 3 with $\nu \sim 2.5$ [12, 13], the leading analytic correction term would have an FSS exponent $\omega_a = 1/\nu \sim 0.4$. The leading correction term estimated from extensive 3d bimodal ISG numerical data analysis [12, 13] has an exponent, $\omega \sim 1.1$, implying a dominant confluent ThL correction with exponent $\theta \sim 2.75$. There is no mention in these publications of any analytic FSS term with an exponent $\omega_a \sim 0.4$. We conclude empirically that quite generally in ISGs the ThL analytic correction terms proportional to τ are small or negligible, presumably due to vanishingly weak prefactors.

Working with the t scaling variable for ISGs as in [12, 20] means that information on critical exponents coming from data temperatures well above criticality is lost. Comments which have been published such as "The difference between the [τ scaling] expressions and the standard expressions is only in the corrections to scaling." [11] or "[The τ scaling] approach might partly take into account the scaling corrections..." [12] are incorrect and follow from a misunderstanding. They refer to the initial lowest order form of τ scaling [17] where corrections to scaling were explicitly left out of the analysis. Full expressions including the Wegner correction terms have been used in the analysis of ferromagnets [22–24] and are used here for ISGs. It is helpful to note that because of exact infinite temperature closure conditions on $\chi(\tau)$, $\xi(\tau)/\beta$, $\gamma(\tau)$ and $\nu(\tau)$ from HTSE, a potentially infinite set of high temperature corrections can generally be grouped together into a single effective correction.

PRIVMAN-FISHER SCALING

The Privman-Fisher FSS ansatz Eq. (24) was originally presented [18] in terms of scaling near criticality, with t as the scaling variable. With the τ scaling expressions the ansatz can be applied successfully over the entire paramagnetic temperature range (see Ref. [23] for a ferromagnet case). Once estimated values for $\beta_c, \gamma, \nu, \theta, a_\chi, a_\xi$ (and possible higher order correction terms if necessary) have been obtained by fits to the ThL regime and extrapolations to criticality, one has explicit expressions for $\chi(\tau, \infty)$ and $\xi(\tau, \infty)$ for the entire paramagnetic regime. Privman-Fisher ansatz [18] scaling plots then can be made for all L and all the paramagnetic regime :

$$\frac{\chi(\tau, L)}{\chi(\tau, \infty)} = F_\chi[L/\xi(\tau, \infty)] + \frac{a_{(\omega,\chi)}}{L^\omega} G_\chi[L/\xi(\tau, \infty)] \quad (24)$$

and

$$\frac{\xi(\tau, L)}{\xi(\tau, \infty)} = F_\xi[L/\xi(\tau, \infty)] + \frac{a_{(\omega,\xi)}}{L^\omega} G_\xi[L/\xi(\tau, \infty)] \quad (25)$$

Scaling, with $\omega = \theta/\nu$, should be "perfect" for all L and over the whole paramagnetic temperature range including the critical FSS regime if the critical parameter estimates have been chosen correctly. This overall scaling can be considered to provide an ultimate validation of the coherence of ThL and FSS fits.

In the case of the Privman-Fisher procedure with τ scaling applied to the cubic Ising ferromagnet susceptibility [23], a simple explicit form for the principal Privman-Fisher scaling function was proposed as a further ansatz:

$$F_\chi(x) = \left(1 - \exp(-bx^{(2-\eta)/a})\right)^a \quad (26)$$

where $x = L/\xi(\beta, \infty)$, and a and b are fit parameters. This extremely compact form automatically fulfils the limit conditions for large and small x. If this ansatz turns out to be generally applicable, the parameters a and b as well as η should be characteristics of a universality class. For the $\xi(\beta, L)$ scaling plot the fit ansatz becomes even simpler :

$$F_\xi(x) = \left(1 - \exp(-bx^{1/a})\right)^a \quad (27)$$

with different a and b parameters. The same approach will be applied below to the ISGs in dimension four.

THE GAUSSIAN ISG IN DIMENSION 4

We will now address the question of specific ISGs in dimension four, starting with the Gaussian interaction distribution. Simulation measurements up to $L = 10$ were published on the 4d Gaussian ISG, together with a 4d bimodal ISG with diluted interactions (65% of the interactions being set to $J = 0$) [14]. The critical temperature for the 4d Gaussian ISG was estimated from Binder parameter and correlation length ratio measurements to be $T_c = 1.805(10)$ so $\beta_c = 0.554(3)$, in agreement with earlier simulation estimates 0.555(3) [38, 39] and consistent with a high temperature series expansion (HTSE) estimate $\beta_c^2 = 0.314(4)$, i.e. $\beta_c = 0.560(4)$ [32]. The simulation analyses [14] led to essentially identical exponents for the two systems : $\nu = 1.02(2)$ and $\eta = -0.275(25)$ and so through scaling rules $\gamma = 2.32(8)$ [14]. The HTSE critical exponent estimates were $\gamma = 2.3(1)$ and $\theta \sim 1.35$ [32]. The two systems of Ref. [14] happen to show small (for the Gaussian) and almost negligible (for the diluted bimodal) corrections to scaling for the Binder parameter, rendering the β_c estimates particularly reliable.

We have repeated the Gaussian measurements of the Binder parameter $g(\beta, L)$ and the correlation length ratio $\xi(\beta, L)/L$, and have also measured the dimensionless parameters $W_q(\beta, L)$, Eq. (4), and $h(\beta, L)$, Eq. (5), in the critical region. Plots of $W_q(\beta, L)$ for chosen fixed β as functions of $L^{-\omega}$ for a fixed ω are shown in Fig. 2, together with fits as described above, Eq. (6). Due to

the weakness of the corrections to scaling for Gaussian interactions (A in Table I) choosing ω to be 1.5, 2.0 or 2.5 made little difference to the output optimal fit parameters. The figures for the other dimensionless parameters are similar and are not presented explicitly for space considerations. The overall fit parameters including uncertainties due to ω are given in Table I.

TABLE I: Values of the 4d Gaussian ISG FSS analysis fit parameters with standard errors. Dimensionless parameters $g(\beta, L)$, $W_q(\beta, L)$, $h(\beta, L)$ and $[\xi/L](\beta, L)$.

$g(\beta_c, \infty)$	0.484	0.003
$A(g)$	0.09	0.04
$B(g)$	0.6028	0.016
$\beta_c(g)$	0.5571	0.0004
$\nu(g)$	1.024	0.013
$W_q(\beta_c, \infty)$	0.248	0.003
$A(W_q)$	0.13	0.03
$B(W_q)$	0.471	0.009
$\beta_c(W_q)$	0.5565	0.0005
$\nu(W_q)$	1.029	0.009
$h(\beta_c, \infty)$	0.394	0.004
$A(h)$	0.11	0.04
$B(h)$	0.578	0.013
$\beta_c(h)$	0.5570	0.0004
$\nu(h)$	1.029	0.015
$[\xi/L](\beta_c, \infty)$	0.451	0.006
$A(\xi/L)$	0.3	0.1
$B(\xi/L)$	0.447	0.009
$\beta_c(\xi/L)$	0.5565	0.0010
$\nu(\xi/L)$	1.03	0.01

We thus obtain consistent estimates, Table I, $\beta_c = 0.557(1)$, $\nu = 1.029(5)$ (taking the average values) together with the infinite size limit dimensionless critical parameter values $g(\beta_c, \infty) = 0.484(3)$, $W_q(\beta_c, \infty) = 0.2418(3)$, $h(\beta_c, \infty) = 0.394(4)$ and $[\xi/L](\beta_c, \infty) = 0.451(6)$. The estimates from the Binder cumulant are in agreement with those of Ref. [14] where $g(\beta_c, \infty) = 0.470(5)$ (no value for $[\xi/L](\beta_c, \infty)$ was cited explicitly and $W_q(\beta, L)$, $h(\beta, L)$ were not measured). The present β_c value is rather more accurate mainly because of a more closely spaced temperature grid and better statistics to higher L. The FSS scaling rule at criticality is $\chi(\beta_c, L) \propto L^{2-\eta}$. Using the present β_c estimate a FSS log-log plot of $\chi(\beta_c, L)/L^2$ against L gives a straight line of slope $-\eta = 0.307(10)$, consistent with the estimate $-\eta = 0.275(25)$ of [14]. From the scaling rule $\gamma = (2-\eta)\nu$ we obtain a FSS estimate $\gamma = 2.35(1)$.

Thermodynamic derivative peak data are shown in the form of peak location $\beta_{\max}(L)$ against inverse peak height $1/D_{\max}(L)$ for the derivatives $\partial g(\beta, L)\partial\beta$, $\partial W_q(\beta, L)/\partial\beta$, and $\partial h(\beta, L)\partial\beta$, Fig. 3. The linear extrapolations to $1/D_{\max}(L) = 0$ lead consistently to $\beta_c = 0.557$, in full agreement with the FSS estimate. Log-log plots of $D_{\max}(L)$ against L have limiting slopes of 0.99(1), so from the scaling rule Eq. (7) $\nu = 1/0.99(1) = 1.01(1)$ again consistent with the FSS estimate. This ν estimate is independent of the estimate for β_c.

The temperature dependent effective exponents $\gamma(\tau, L)$ and $\nu(\tau, L)$, Eqs. (10), (18) assuming $\beta_c = 0.557$ are shown in Figs. 4 and 5. The ThL regime can be recognized by the condition $\gamma(\tau, L)$ or $\nu(\tau, L)$ becoming independent of L, or from the figure of merit Eq. (22). The ThL regime correlation length exponent $\nu(\tau)$ has only a weak temperature variation. The overall fit to the $\nu(\tau, L)$ data in Fig. 5 gives a ThL temperature dependent exponent

$$\nu(\tau) = 1.032 - \frac{0.041 \cdot 1.6\,\tau^{1.6} + 0.017 \cdot 3\,\tau^3}{1 + 0.041\,\tau^{1.6} + 0.017\,\tau^3} \qquad (28)$$

or

$$\xi(\beta, \infty) = 0.95\beta\tau^{-1.032}\left(1 + 0.041\,\tau^{1.6} + 0.017\,\tau^3\right) \quad (29)$$

so with $\nu = 1.032(5), \theta \sim 1.6, a_\xi = 0.041(5)$ and a weak higher order contribution. The correction exponent estimate $\theta \sim 1.6$ is compatible with the HTSE value $\theta \sim 1.35$ [32].

The $\gamma(\tau)$ curve evaluated directly from the HTSE series [32] is exact at high and moderate temperatures, once β_c is estimated, and is fully consistent with the ThL $\gamma(\tau, L)$ simulation data in the appropriate τ range, Fig. 4 (Fig. 1 and Fig. 4 are alternative presentations of the same derivative data). The simulation and HTSE data taken together show that for the leading confluent correction term $\tau(\theta)$ the prefactor is small, and that there is a weak high order effective correction term, so

$$\gamma(\tau) = 2.44 - \frac{0.06 \cdot 1.6\,\tau^{1.6} - 0.017 \cdot 8\,\tau^8}{1 + 0.06\,\tau^{1.6} - 0.017\,\tau^8} \qquad (30)$$

i.e.

$$\chi(\beta, \infty) = 0.96\,\tau^{-2.44}\left(1 + 0.06\,\tau^{1.6} - 0.017\,\tau^8\right) \quad (31)$$

Hence $\gamma = 2.44(2)$, $\theta_{\text{eff}} \sim 1.6$ and $a_\chi = 0.06(1)$. From the extrapolated derivative $\partial \ln \chi(\beta, L)/\partial \ln(\xi(\beta, L)/\beta)$, Fig. 6, $\eta = -0.36(4)$. This estimate is independent of the estimate for β_c.

These critical exponents : $\nu = 1.032(5)$, $\gamma = 2.43(2)$, $\eta = -0.36(4)$ estimated from the ThL data are thus in full agreement with the FSS estimates above, and with the slightly less precise FSS estimations of Ref. [14] : $\nu = 1.02(2)$, $\gamma = 2.32(8)$, $\eta = -0.275(25)$. The observed exponents $\gamma = 2.43(2)$ and $\theta \sim 1.6$ are also consistent with the HTSE estimates $\gamma = 2.3(1)$ and $\theta \sim 1.35$ [32]. There is thus excellent overall consistency. The critical temperature and exponent values are particularly reliable in this model because of the accidental weakness of the correction to scaling terms.

With the ThL $\chi(\beta, \infty)$ and $\xi(\beta, \infty)$ expressions in hand we make up the Privman-Fisher susceptibility plot $\chi(\beta, L)/\chi(\beta, \infty) = F_\chi[L/\xi(\beta, \infty)]$, Fig. 7. The whole data set for the entire paramagnetic temperature region

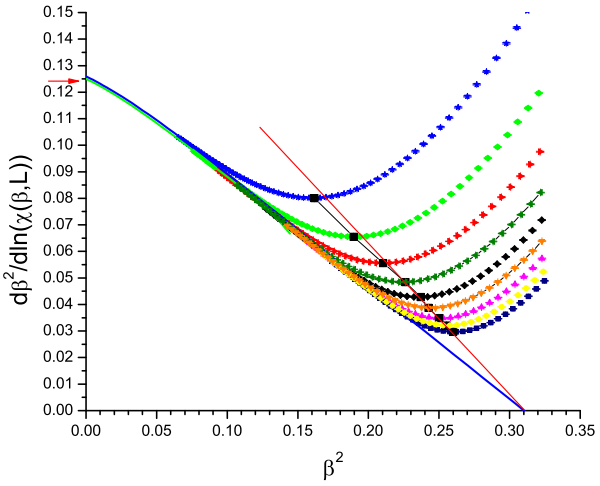

FIG. 1: (Color online) The 4d Gaussian derivatives $\partial\beta^2/\partial \ln \chi(\beta, L)$ as a function of β^2. Throughout the paper, the symbol code for sizes is : $L = 14$ purple pentagons, $L = 13$ wine stars, $L = 12$ navy squares, $L = 11$ yellow hexagons, $L10$ pink circles,$L = 9$ orange balls, $L = 8$ black triangles, $L = 7$ olive inverted triangles, $L = 6$ red diamonds, $L = 5$ green left triangles, $L = 4$ blue right triangles. (For display purposes not all sizes are shown in each Figure). Blue curve : ThL regime data fit. Large squares : minima locations for each L, straight line : extrapolation to β_c^2.

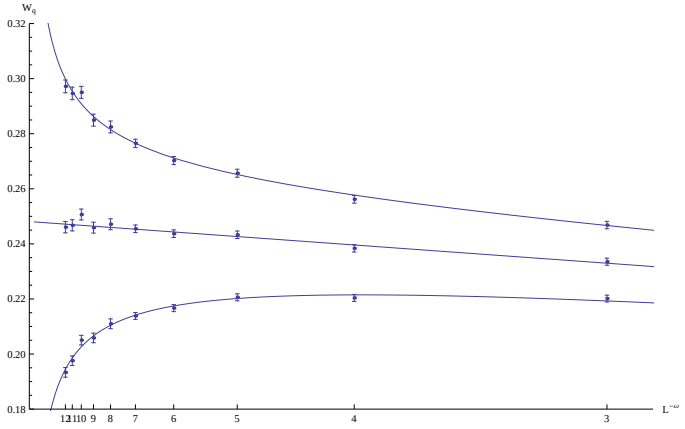

FIG. 2: (Color online) The 4d Gaussian W_q finite size scaling. Data and fit curves : upper $\beta = 0.5665$, centre $\beta = 0.5565$, lower $\beta = 0.5465$. Fit value $\omega = 2$. See text and Table I.

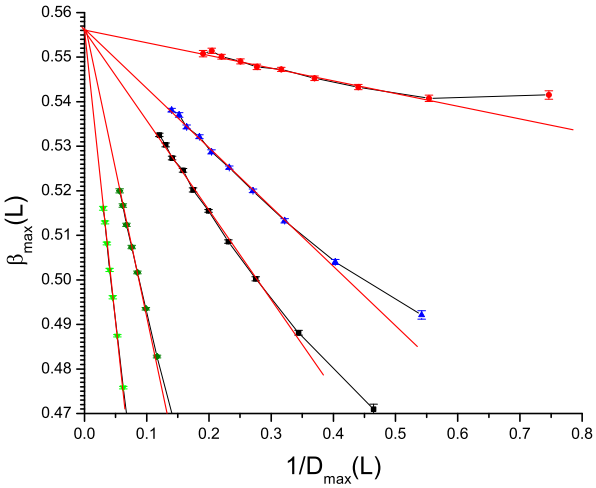

FIG. 3: (Color online) The 4d Gaussian thermodynamic derivative peaks; peak location $\beta_{\max}(L)$ as function of inverse peak heights $1/D(L)$ where $D(L) = \max \partial U(\beta, L)/\partial\beta$. Observables U: red circles W_q, blue triangles h, black squares g, green inverted triangles $\ln \chi$, olive diamonds $\ln |q|$. Straight line fits indicate extrapolations to β_c (see text).

and all L (so covering the FSS regime, the ThL regime, and the intermediate regime) shows an excellent scaling, which can be fitted by the ansatz Eq. (26) using the fit parameters $\eta = -0.36(3)$, $a = 1.89(2)$, $b = 0.43(2)$. The Privman-Fisher correlation length plot can be fitted with parameters $a = 0.80(2)$ and $b = 0.35(2)$ in Eq. (27). There is a small finite size scaling correction which we have not attempted to analyse.

We have no data for the diluted bimodal ISG of Ref. [14] but in view of the fact that the FSS data in that model displayed the figures show even weaker corrections to scaling than for the Gaussian, the exponent and dimensionless parameter estimates $\nu = 1.025(15)$, $\gamma = 2.33(6)$, $\eta = -0.275(25)$, $g(\beta_c) = 0.472(2)$ are certainly very reliable also.

THE LAPLACIAN INTERACTION ISG IN DIMENSION 4

Simulation data were obtained for the Laplacian interaction ISG, $P(J) \propto \exp(-|J|)$, in dimension 4 with the same method and analyses as for the Gaussian, and with 2^{13} samples for each size L up to $L = 12$. The FSS of the $W_q(\beta, L)$ data, Fig. 9, showed negligible corrections to scaling, and the other dimensionless parameters showed only very weak corrections. In consequence β_c, ν, and the critical values of the dimensionless parameters could be estimated rather precisely, Table II. The thermodynamic peak location data, Fig. 10, extrapolate to a β_c estimate which is consistent with the FSS estimate. The susceptibility and correlation length ThL measurements give estimates of the critical exponents γ and ν which are also in full agreement with the FSS and pseudo-critical peak data, see Fig. 11 and Fig. 12. They also show weak correction term factors.

The overall conclusions from the analyses for the Laplacian are : $\beta_c = 0.6221(5)$, with critical exponents $\nu = 1.026(5)$, $\gamma = 2.385(10)$, $\eta = -0.32(4)$ and criti-

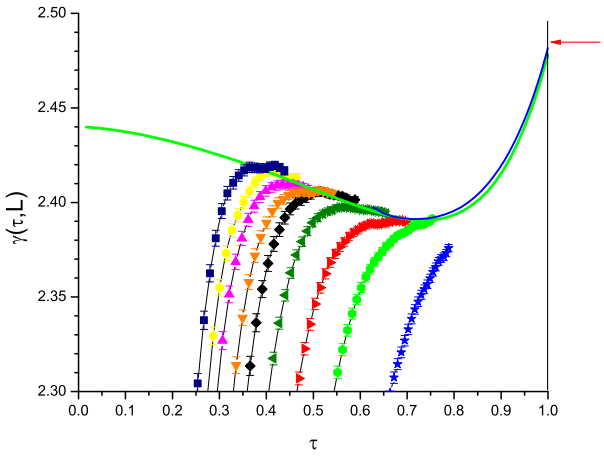

FIG. 4: (Color online) The 4d Gaussian temperature dependent effective exponent $\gamma(\tau) = \partial\chi(\beta, L)/\partial\tau$ for $\beta_c = 0.557$. Symbol code as in Fig. 1. Blue curve : HTSE data points. Green curve : ThL regime data fit.

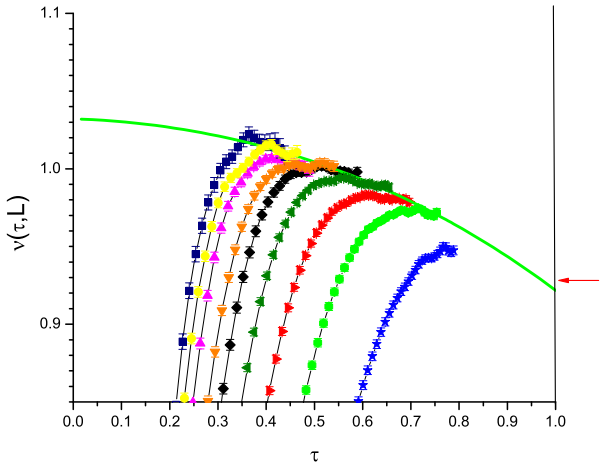

FIG. 5: (Color online) The 4d Gaussian effective $\nu(\tau) = \partial(\xi(\beta, L)/\beta)/\partial\tau$ for $\beta_c = 0.557$. Symbol code as in Fig. 1. Blue curve : ThL regime data fit.

cal values for the dimensionless parameters $g(\beta_c, \infty) = 0.4747(6)$, $W_q(\beta_c, \infty) = 0.2385(4)$, $h(\beta_c, \infty) = 0.385(1)$, and $[\xi/L](\beta_c, \infty) = 0.446(1)$. For all the parameters the correction exponent θ or ω values are large, we have used $\omega = 3 \pm 1$ for the fits and error estimates. As these are effective exponents the values are not the same for all the parameters. The overall fit to the $\chi(\tau, L)$ data with the leading correction term is $\chi(\tau, \infty) = 1.14\tau^{-2.385}(1 - 0.12\tau^5)$. The overall fit to the $\xi(\tau, L)$ data with a leading and a high order correction term is

$$\xi(\tau, \infty) = 0.90\,\beta\,\tau^{-1.02}(1 + 0.1\,\tau^{1.7} + 0.007\,\tau^{10}) \quad (32)$$

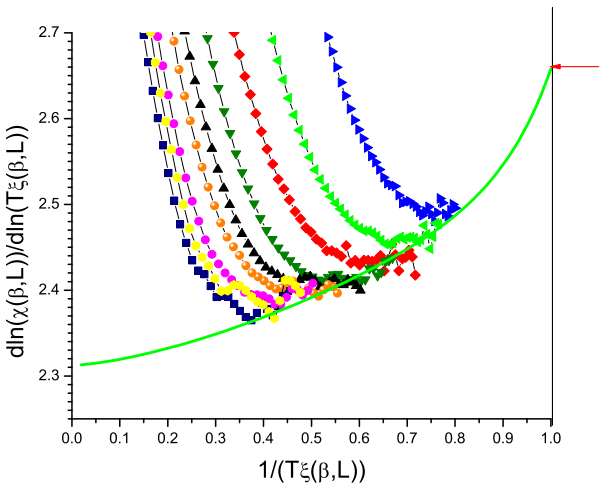

FIG. 6: (Color online) The 4d Gaussian effective exponent $2 - \eta(\beta) = \partial \ln\chi(\beta, L)/\partial \ln(\xi(\beta, L)/\beta)$ against $\beta/\xi(\beta, L)$. Symbol code as in Fig. 1. Green envelope curve : ThL regime data fit and extrapolation.

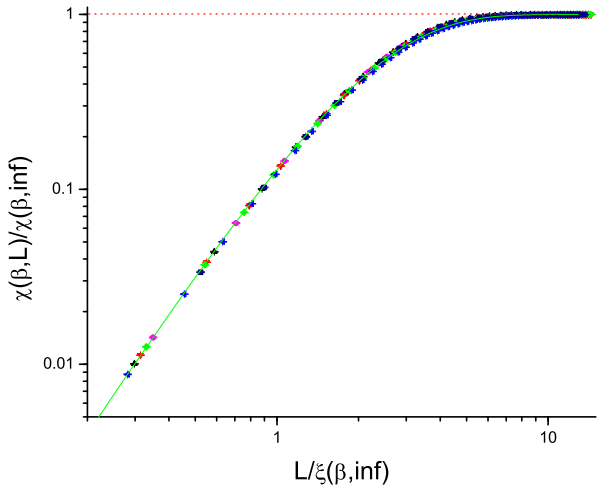

FIG. 7: (Color online) The 4d Gaussian Privman-Fisher χ FSS plot, $\chi(\tau, L)/\chi(\tau, \infty)$ against $L/\xi(\tau, \infty)$ where $\chi(\tau, \infty)$ and $\xi(\tau, \infty)$ are fit and extrapolation values from the $\gamma(\tau)$ and $\nu(\tau)$ analyses. Symbol code as in Fig. 1. Curve : fit (see text)

The Privman-Fisher FSS fit Eq. (26), Fig. 14, is

$$\frac{\chi(\tau, L)}{\chi(\tau, \infty)} = \left(1 - \exp\left[-0.38\left(\frac{L}{\xi(\tau, \infty)}\right)^{\frac{2.3}{1.75}}\right]\right)^{1.75} \quad (33)$$

TABLE II: Values of the 4d Laplacian ISG FSS analysis fit parameters with standard errors. Dimensionless parameters $g(\beta, L)$, $W_q(\beta, L)$, $h(\beta, L)$ and $[\xi/L](\beta, L)$.

$g(\beta_c, \infty)$	0.4747	0.0006
$A(g)$	−0.006	0.02
$B(g)$	0.51	0.02
$\beta_c(g)$	0.6226	0.0001
$\nu(g)$	1.02	0.01
$W_q(\beta_c, \infty)$	0.2385	0.0004
$A(W_q)$	−0.15	0.01
$B(W_q)$	0.39	0.01
$\beta_c(W_q)$	0.6215	0.0010
$\nu(W_q)$	1.02	0.01
$h(\beta_c, \infty)$	0.385	0.001
$A(h)$	0.060	0.015
$B(h)$	0.48	0.01
$\beta_c(h)$	0.6223	0.0004
$\nu(h)$	1.026	0.010
$[\xi/L](\beta_c, \infty)$	0.446	0.001
$A(\xi/L)$	0.65	0.10
$B(\xi/L)$	0.38	0.01
$\beta_c(\xi/L)$	0.6220	0.0003
$\nu(\xi/L)$	1.03	0.01

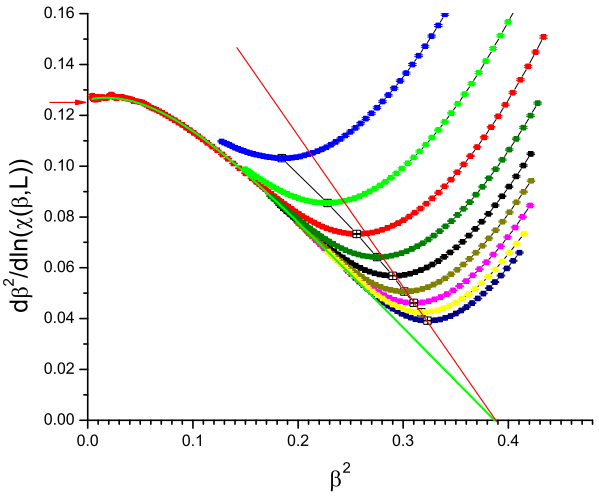

FIG. 8: (Color online) The 4d Laplacian derivatives $\partial\beta^2/\partial \ln \chi(\beta, L)$ as a function of β^2. Throughout the paper, the symbol code for sizes is as in Fig. 1. Blue curve : ThL regime data fit. Green curve: ThL regime envelope fit. Large squares : minima locations for each L. Straight line : extrapolation to β_c^2.

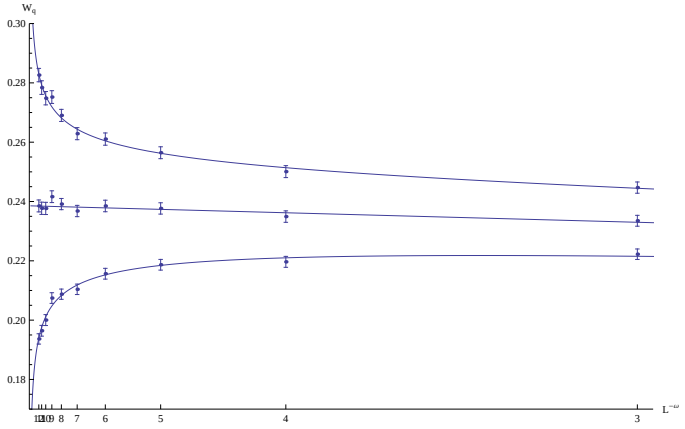

FIG. 9: (Color online) The 4d Laplacian W_q finite size scaling. Data and fit curves : upper $\beta = 0.6315$, centre $\beta = 0.6215$, lower $\beta = 0.6115$. Fit value $\omega = 3$. See text and Table II.

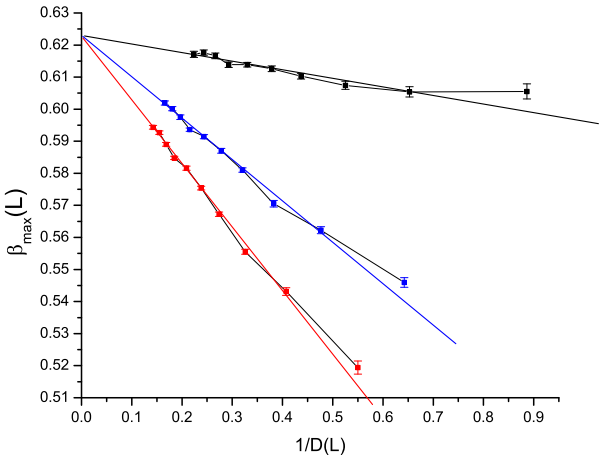

FIG. 10: (Color online) The 4d Laplacian thermodynamic derivative peaks; peak location $\beta_{\max}(L)$ as function of inverse peak heights $1/D_{\max}(L)$ where $D_{\max}(L) = \max \partial U(\beta, L)/\partial\beta$. Observables U: red circles W_q, blue triangles h, black squares g, Straight line fits indicate extrapolations to β_c (see text).

THE BIMODAL ISG IN DIMENSION 4

For the 4d bimodal ISG, from early simulation measurements up to $L = 10$ a critical temperature $\beta_c = 0.493(7)$ (i.e. $\beta_c^2 = 0.243(7)$) was estimated [41] using the Binder parameter crossing point criterion. However, finite size corrections to scaling were not allowed for. The exponent estimates were $\nu = 1.0(1)$ and $\eta = -0.30(5)$. Extensive domain wall free energy measurements to $L = 10$ gave an estimate $\beta_c = 0.50(1)$ (i.e. $\beta_c^2 = 0.25(1)$) [42]. Inspection of the raw data [43] shows strong finite size corrections; extrapolation to larger L leads to an infinite size limit β_c definitely greater than 0.50. The HTSE critical temperature and exponent estimates are [32] $\beta_c^2 = 0.26(2)$ (i.e. $\beta_c = 0.51(2)$), $\gamma = 2.5(3)$ and a leading confluent correction exponent $\theta \sim 1.5$.

From bimodal 4d simulations with impressive numbers of samples up to $L = 16$ and to a maximum inverse temperature $\beta = 0.5025$, Baños *et al.* [20] give estimates $\omega = 1.04(10)$, $\nu = 1.068(7)$ (so $\theta = \omega\nu = 1.11(12)$), $\eta = -0.320(13)$ (so $\gamma = (2 - \eta)\nu = 2.48(3)$) and

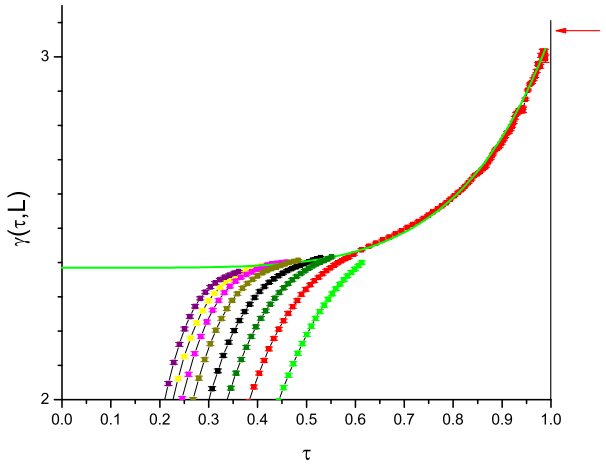

FIG. 11: (Color online) The 4d Laplacian temperature dependent effective exponent $\gamma(\tau) = \partial\chi(\beta, L)/\partial\tau$ for $\beta_c = 0.662$. Symbol code as in Fig. 1. Green curve : ThL regime envelope fit.

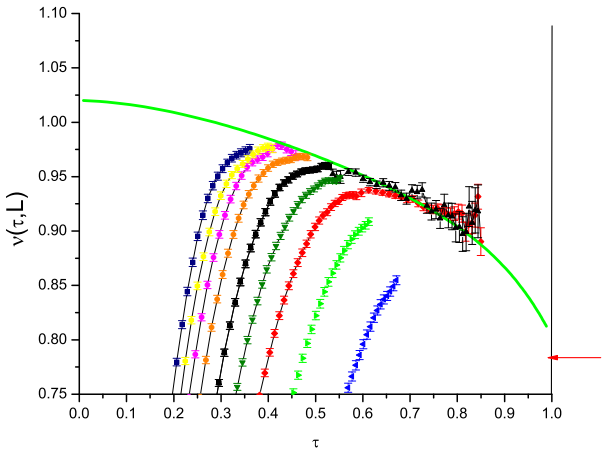

FIG. 12: (Color online) The 4d Laplacian effective exponent $\nu(\tau) = \partial(\xi(\beta, L)/\beta)/\partial\tau$ with $\beta_c = 0.662$. Symbol code as in Fig. 1. Green curve : ThL regime data fit.

$\beta_c = 0.5023(6)$, all from a FSS analysis with t as scaling variable. We can note that the inverse temperatures for the $(U_4(\beta, L), U_4(\beta, 2L))$ and $([\xi/L](\beta, L), [\xi/L](\beta, 2L))$ crossing points should scale linearly with $1/L^{\omega+1/\nu}$, Eq. 30 of [20]. However, it can be seen that in the crossing point plot, Fig. 9 of Ref. [20], with the authors' preferred values of ω and ν the scaling against $1/L^{\omega+1/\nu}$ is far from being linear. Baños *et al.* obtain fits by discarding the lower L points or by introducing strong higher order terms. An alternative explanation could be that despite the precautions taken complete equilibration has not quite been achieved for the largest β measurements

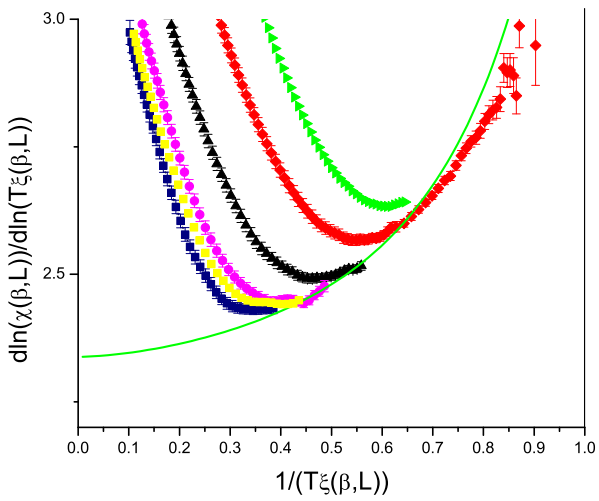

FIG. 13: (Color online) The 4d Laplacian effective exponent $2-\eta(\beta) = \partial \ln\chi(\beta, L)/\partial \ln(\xi(\beta, L)/\beta)$ against $\beta/\xi(\beta, L)$. Symbol code as in Fig. 1. Green envelope curve : ThL regime data fit and extrapolation.

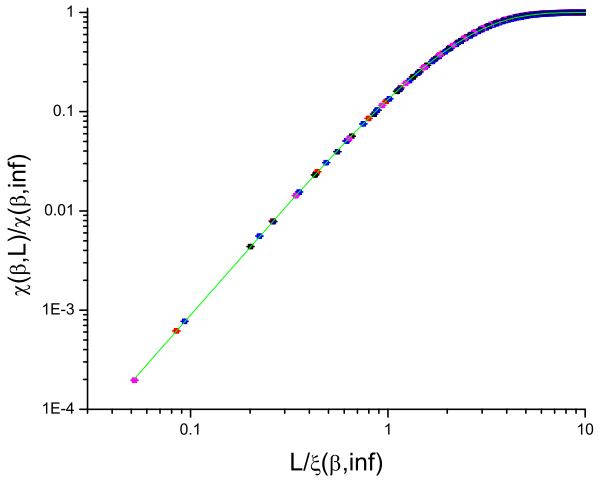

FIG. 14: (Color online) The 4d Laplacian Privman-Fisher χ FSS plot, $\chi(\tau, L)/\chi(\tau, \infty)$ against $L/\xi(\tau, \infty)$ where $\chi(\tau, \infty)$ and $\xi(\tau, \infty)$ are fit and extrapolation values from the $\gamma(\tau)$ and $\nu(\tau)$ analyses. Symbol code as in Fig. 1. Curve : fit (see text)

at the largest size $L = 16$ (where equilibration is the most difficult), so the $L = 16$ to $L = 8$ crossing points could be dropped. In this case the remaining data points appear more consistent and indicate a rather larger critical inverse temperature β_c and a rather larger $\omega+1/\nu$. Our independent data reported below are compatible with these modified values.

We have made measurements in the critical region of

the standard finite size Binder cumulant $g(\beta, L)$, the dimensionless parameters $W_q(\beta, L)$ and $h(\beta, L)$, and the normalized correlation length $[\xi/L](\beta, L)$. The present data are for all L from 3 to 14 and span the estimated inverse critical temperature β_c. From fits to the $g(\beta, L)$, $W_q(\beta, L)$, and $h(\beta, L)$ we obtain FSS estimates for the critical temperature β_c and the exponent ν together with the dimensionless critical values $g(\beta_c, \infty)$, $W_q(\beta_c, \infty)$, see Fig. 16, and $h(\beta_c, \infty)$. The correlation length ratio $[\xi/L](\beta, L)$ has much larger corrections to scaling than the other observables, so the data for this parameter was not readily exploitable. As explained above rather than following the traditional crossing point analysis, the raw dimensionless parameter data are fitted directly to Eq. (6) at fixed temperatures in the critical region. Consistent independent fits could be made to the $g(\beta, L)$, $W_q(\beta, L)$ and $h(\beta, L)$ results for the data from $L = 4$ to $L = 14$. (To minimize higher order corrections we have eliminated $L = 3$ from the fitting process). Fits were made fixing the correction exponent at three alternative values, $\omega = 1.0$, 1.3 and 1.6. The fit values with error bars which include the effect of the assumed uncertainty in ω are given in Table III.

TABLE III: Values of the 4d bimodal ISG FSS analysis fit parameters with standard errors. Dimensionless parameters $g(\beta, L)$, $W_q(\beta, L)$, $h(\beta, L)$ and $[\xi/L](\beta, L)$.

$g(\beta_c, \infty)$	0.5258	0.0055
$A(g)$	−0.2089	0.026
$B(g)$	0.7485	0.037
$\beta_c(g)$	0.5058	0.0007
$\nu(g)$	1.08	0.03
$W_q(\beta_c, \infty)$	0.2789	0.0031
$A(W_q)$	−0.1820	0.015
$B(W_q)$	0.5883	0.021
$\beta_c(W_q)$	0.5045	0.0005
$\nu(W_q)$	1.07	0.02
$h(\beta_c, \infty)$	0.435	0.010
$A(h)$	−0.215	0.025
$B(h)$	0.7199	0.023
$\beta_c(h)$	0.5056	0.0006
$\nu(h)$	1.09	0.02
$[\xi/L](\beta_c, \infty)$	0.4780	0.0028
$A(\xi/L)$	−0.2925	0.014
$B(\xi/L)$	0.5111	0.019
$\beta_c(\xi/L)$	0.5036	0.0005
$\nu(\xi/L)$	1.02	0.02

Estimates for the important critical values of the dimensionless parameters for 4d bimodal ISG are not quoted explicitly in Ref. [20], but a limit $U_4(\beta_c) < 2.00$ i.e. $g(\beta_c, \infty) > 0.50$ can be read off the appropriate figure. From the present bimodal analysis, $g(\beta_c, \infty) = 0.526(6)$ (or $U_4(\beta_c, \infty) = 1.948(12)$), $W_q(\beta_c, \infty) = 0.279(3)$ and $h(\beta_c, \infty) = 0.435(10)$.

Thermodynamic derivative peak data are shown in Fig. 17. The straight line extrapolations of peak locations $\beta_{\max}(L)$ against the inverse peak strengths $1/\max[\partial U(\beta, L)/\partial\beta]$ for observables $U(\beta, L)$ show consistently $\beta_{\max}(L)$ values tending to a $\beta_c = 0.5050(5)$ in the infinite L limit. Log-log plots of $\max[\partial U(\beta, L)/\partial\beta]$ versus L tend to straight lines with limiting slopes $1/\nu$ corresponding to $\nu = 1.12(2)$. It should be again underlined that these estimates for ν are independent of the β_c estimates.

We show in Fig. 18 and Fig. 19 $\gamma(\tau, L)$ and $\nu(\tau, L)$ plots for 4d binomial ISG using as the inverse critical temperature $\beta_c = 0.505$ as estimated from the FSS and thermodynamic peak analyses. Satisfactory fits can be obtained with $\nu = 1.14(2)$, $\theta \sim 1.8$, and $\gamma = 2.76(3)$ with prefactors $a_\xi = 0.10, a_\chi = 0.69$ and a weak high order correction term for $\gamma(\tau)$, $y \sim 8, b_\chi \sim -0.01$. There is consistency between the FSS exponent estimates and the ThL estimates.

In Ref [20], the FSS estimate of the bimodal ISG critical temperature is $\beta_c = 0.5023(6)$. Fixing β_c at this value, a ThL $\gamma(\tau)$ fit leads to an estimate $\gamma = 2.60(3)$, still considerably above the Gaussian value. However, the fit requires a correction exponent $\theta \sim 2.0$, corresponding to $\omega \sim 1.8$, which is considerably higher than the Ref. [20] FSS value $\omega = 1.04(10)$.

Finally Privman-Fisher ansatz plots can be made up for all the data. Assuming $\beta_c = 0.505$ and the fit parameters from the $\gamma(\tau, L)$ and $\nu(\tau, L)$ plots, the Privman-Fisher scaling is shown in Fig. 21. It can be seen that the χ scaling is excellent on the scale of the figure over the entire range of paramagnetic temperatures and of sizes. The scaling curve can be fitted accurately by the explicit form used to fit the simple cubic Ising ferromagnet data, Eq. (26) with $\eta = -0.40$, $a = 1.95$, and $b = 0.43$ for the χ scaling plot. For the ξ scaling plot a good large L fit is obtained using the ansatz Eq. (27) with $a = 0.74$, and $b = 0.35$ with indications of finite size corrections which we have not attempted to analyse. It can be noted that both for χ and ξ the values of the fit parameters (which should be characteristic of a universality class) obtained for the bimodal, Gaussian and Laplacian ISGs are not quite identical.

The present critical exponents γ for both the bimodal and Gaussian ISGs are consistent with, but are more accurate than, the HTSE estimates, principally because the uncertainty in β_c^2 is considerably reduced thanks to the FSS and thermodynamic analyses of the simulation data. The 4d bimodal γ and ν exponent estimates can be compared to the values found above for the 4d Gaussian, and with the published estimates Gaussian and diluted bimodal systems [14]. The critical exponents of the 4d bimodal ISG are well above those of the 4d Gaussian and diluted bimodal ISGs.

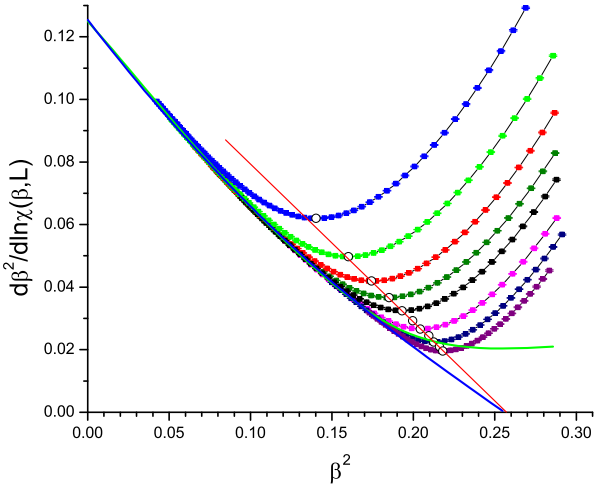

FIG. 15: (Color online) The 4d bimodal derivatives $\partial\beta^2/\partial \ln\chi(\beta, L)$ as a function of β^2. Symbol code as in Fig. 1. Green curve : ThL derivative from the 15 exact term HTSE series [32]. Blue curve : ThL regime data fit and extrapolation. Open circles : minima locations for each L, straight line : extrapolation to β_c^2.

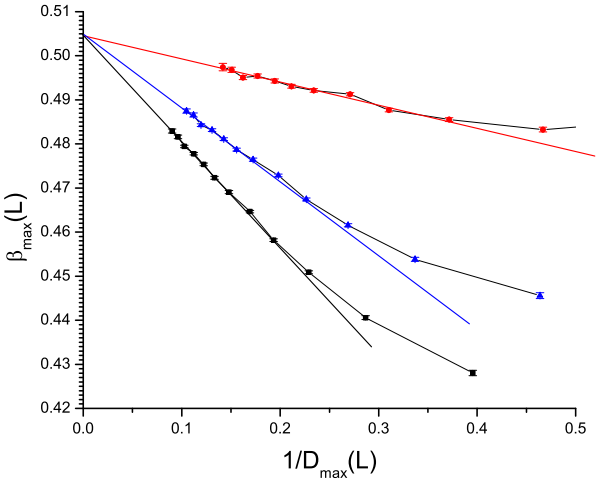

FIG. 17: (Color online) The 4d bimodal thermodynamic derivative peaks; peak location $\beta_{\max}(L)$ as function of inverse peak heights $1/D_{\max}(L)$ where $D_{\max}(L) = \max \partial U(\beta, L)/\partial\beta$. Observables U: red circles W_q, blue triangles h, black squares g. Straight line fits indicate extrapolations to β_c (see text).

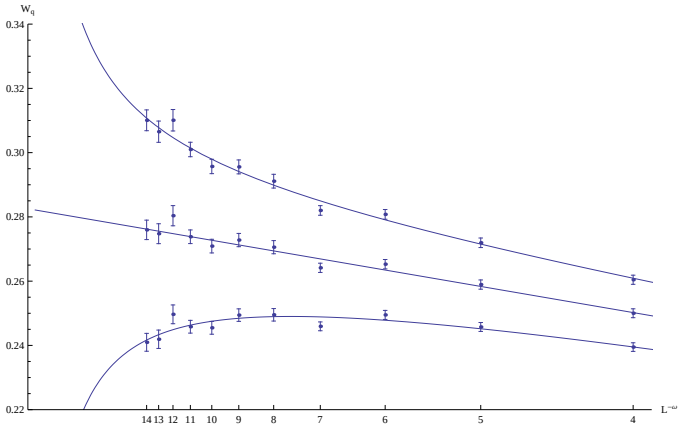

FIG. 16: (Color online) The 4d bimodal W_q finite size scaling. Data and fit curves : upper $\beta = 0.51032$, center $\beta = 0.50532$, lower $\beta = 0.50032$. Fit value $\omega = 1.3$. See text and Table III.

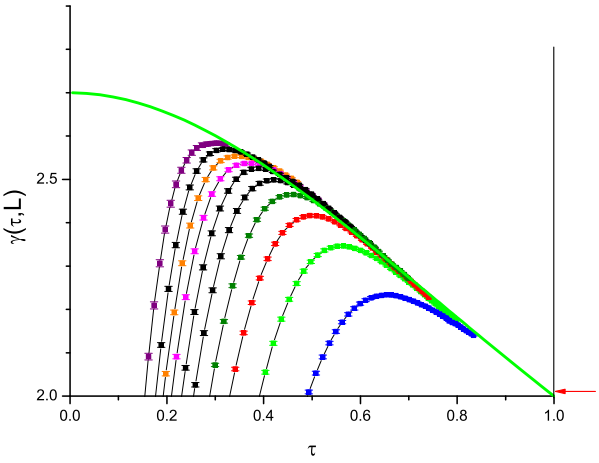

FIG. 18: (Color online) The 4d bimodal temperature dependent effective exponent $\gamma(\tau) = \partial\chi(\beta, L)/\partial\tau$ for $\beta_c = 0.505$. Symbol code as in Fig. 1. Green curve : HTSE data points. Blue curve : ThL regime data fit.

COMPARISONS BETWEEN MODELS

The bimodal, Gaussian, Laplacian and diluted bimodal infinite size limit critical values for the Binder cumulant can be compared:

- bimodal $g(\beta_c, \infty) = 0.526(5)$ (or > 0.500 [20]),
- Gaussian $g(\beta_c, \infty) = 0.484(3)$ (or 0.470(5) [14]),
- Laplacian $g(\beta_c, \infty) = 0.4747(6)$
- diluted $g(\beta_c, \infty) = 0.472(2)$ [14].

The value estimated for the bimodal model is strikingly different from those for the other models. Given the high precision of the other estimates it would appear that they are not quite identical to each other either. For the other dimensionless parameters (measurements have been made only in the present work)

- bimodal $W_q(\beta_c, \infty) = 0.279(3)$
- Gaussian $W_q(\beta_c, \infty) = 0.248(3)$

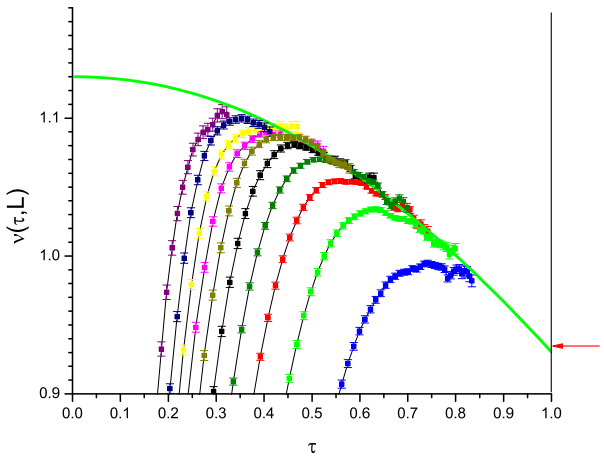

FIG. 19: (Color online) The 4d bimodal effective $\nu(\tau) = \partial(\xi(\beta,L)/\beta)/\partial\tau$ for $\beta_c = 0.505$. Symbol code as in Fig. 1. Green curve : ThL regime data fit.

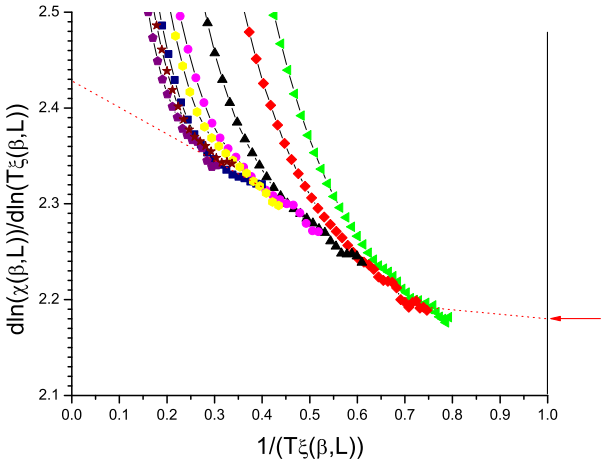

FIG. 20: (Color online) The 4d bimodal effective exponent $2 - \eta(\beta) = \partial \ln \chi(\beta,L)/\partial \ln(\xi(\beta,L)/\beta)$ against $\beta/\xi(\beta,L)$. Symbol code as in Fig. 1. Dotted envelope curve : ThL regime data fit and extrapolation.

- Laplacian $W_q(\beta_c,\infty) = 0.2385(4)$

and

- bimodal $h(\beta_c,\infty) = 0.435(10)$
- Gaussian $h(\beta_c,\infty) = 0.394(4)$,
- Laplacian $h(\beta_c,\infty) = 0.385(1)$.

The distinction between the bimodal value and the other two values is again very significant. As the critical limit values of dimensionless parameters are characteristic of a university class, even without knowing the

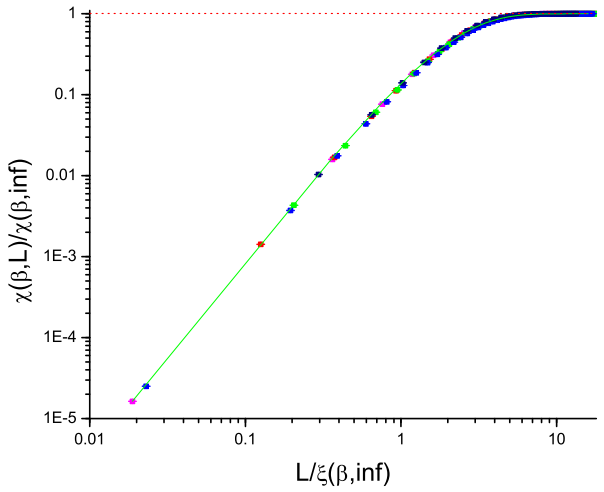

FIG. 21: (Color online) The 4d bimodal Privman-Fisher χ FSS plot, $\chi(\tau,L)/\chi(\tau,\infty)$ against $L/\xi(\tau,\infty)$ where $\chi(\tau,\infty)$ and $\xi(\tau,\infty)$ are fit and extrapolation values from the $\gamma(\tau)$ and $\nu(\tau)$ analyses. Symbol code as in Fig. 1. Curve : fit (see text)

critical exponents these model-to-model differences already clearly demonstrate that the 4d binomial ISG is not in the same universality class as the other three 4d ISG models.

The critical exponents from a combination of FSS, thermodynamic peak, and ThL information (when available) are

- bimodal $\gamma(\beta_c,\infty) = 2.70(4)$,
- Gaussian $\gamma(\beta_c,\infty) = 2.44(4)$,
- Laplacian $\gamma(\beta_c,\infty) = 2.40(2)$,
- diluted $\gamma(\beta_c,\infty) = 2.33(6)$ [14]

and

- bimodal $\nu(\beta_c,\infty) = 1.13(1)$,
- Gaussian $\nu(\beta_c,\infty) = 1.030(5)$,
- Laplacian $\nu(\beta_c,\infty) = 1.020(5)$
- diluted $\nu(\beta_c,\infty) = 1.025(15)$ [14]

The two critical exponents γ and ν for the bimodal interaction model are both much higher than the values for the Gaussian, Laplacian, and diluted bimodal interaction models.

CONCLUSIONS

Simulations on the 4d Gaussian, Laplacian and bimodal ISGs up to size $L = 12$ and $L = 14$ respectively

are first analysed in the critical temperature range to obtain estimates for the critical inverse temperatures β_c, together with FSS estimates for the critical values for dimensionless parameters $g(\beta_c, \infty)$, $W_q(\beta_c, \infty)$ of Eq. (4) and $h(\beta_c, \infty)$ of Eq. (5), and for the anomalous and correlation length critical exponents η and ν. The thermal derivative peak method has been used to obtain complementary estimates for β_c, and independent estimates of the critical exponent ν which are not dependent on the β_c estimates. The critical temperatures β_c are consistent with the FSS estimates and are in full agreement with, but are more precise than, the estimates from high temperature scaling expansions alone [32]. They also improve on previous FSS numerical estimates [14, 20].

We spell out in detail the procedure used for scaling over the whole paramagnetic temperature range with the appropriate ISG scaling variable, $\tau = 1 - (\beta/\beta_c)^2$, together with scaling expressions which include the correction terms, Eqs. (16) and (17).

With the estimates for β_c in hand, data for the temperature dependent effective exponents $\gamma(\tau)$ and $\nu(\tau)$ in the thermodynamic limit (ThL) regime were fitted and extrapolated to obtain critical exponent γ, ν and θ estimates together with the strengths of the correction terms. There is consistency between the FSS, thermodynamic derivative peak, and ThL estimates for each model. Overall Privman-Fisher scalings with the estimated critical parameters, covering the whole paramagnetic temperature range and all sizes L, validate the analysis.

The critical values of the dimensionless parameters and the critical exponents are characteristic of a universality class. For each of the recorded observables the values for the 4d bimodal ISG are quite different from those of the 4d Gaussian ISG and the 4d Laplacian (or from those of the 4d diluted bimodal ISGs [14]), showing that these systems lie in different universality classes. It can be concluded that for ISG transitions in dimension 4 at least, and probably more generally [36, 37], the critical parameters depend on the form of the interaction distribution, so the standard RGT universality rules do not apply.

ACKNOWLEDGEMENTS

We are very grateful to Koji Hukushima for important comments and communication of unpublished data. We thank Amnon Aharony for constructive criticism. The computations were performed on resources provided by the Swedish National Infrastructure for Computing (SNIC) at the High Performance Computing Center North (HPC2N) and Chalmers Centre for Computational Science and Engineering (C3SE).

[1] R. Baxter, Phys. Rev. Lett. **26**, 832 (1971)
[2] L. P. Kadanoff and F. J. Wegner, Phys. Rev. B **4**, 3989 (1971).
[3] H. E. Stanley, Rev. Mod. Phys. **71**, S358 (1999)
[4] E. Gardner, J. Phys. **45**, 1755 (1984).
[5] G. Parisi, R. Petronzio, and F. Rosati, Eur. Phys. J. B **21**, 605 (2001)
[6] M. Castellana, Eur. Phys. Lett. **95**, 47014 (2011)
[7] M. C. Angelini, G. Parisi, and F. Ricci-Tersenghi, Phys. Rev. B **87**, 134201 (2013)
[8] S. Gartenhaus and W. S. McCullough, Phys. Rev. B **38**, 11688 (1988).
[9] H. G. Katzgraber, I. A. Campbell, and A. K. Hartmann, Phys. Rev. B **78**, 184409 (2008).
[10] R. N. Bhatt and A. P. Young, Phys. Rev. B **37**, 3707 (1988).
[11] H. G. Katzgraber, M. Korner, and A. P. Young, Phys. Rev. B **73**, 224432 (2006).
[12] M. Hasenbusch, A. Pelissetto, and E. Vicari, Phys. Rev. B **78**, 214205 (2008).
[13] M. Baity-Jesi *et al.*, Phys. Rev. B **88**, 224416 (2013).
[14] T. Jörg and H. G. Katzgraber, Phys. Rev. B **77**, 214426 (2008).
[15] T. Jörg and H. G. Katzgraber, Phys. Rev. Lett. **101**, 197205 (2008).
[16] We will use the inverse temperature $\beta = 1/T$ or its square throughout.
[17] I. A. Campbell, K. Hukushima, and H. Takayama, Phys. Rev. Lett. **97**, 117202 (2006).
[18] V. Privman and M. E. Fisher, Phys. Rev. B **30**, 322 (1984).
[19] I. A. Campbell and D. C. M. C. Petit, J. Phys. Soc. Japan, **79**, 011006 (2010).
[20] R. A. Baños, L. A. Fernandez, V. Martin-Mayor, and A. P. Young, Phys. Rev. B **86**, 134416 (2012).
[21] F. Wegner, Phys. Rev. B **5**, 4529 (1972).
[22] I. A. Campbell and P. Butera, Phys. Rev. B **78**, 024435 (2008).
[23] I. A. Campbell and P. H. Lundow, Phys. Rev. B **83**, 014411 (2011).
[24] P. H. Lundow and I. A. Campbell, Phys. Rev. B **83**, 184408 (2011).
[25] E. Luijten, H. W. J. Blöte, and K. Binder, Phys. Rev. Lett. **79**, 561 (1997).
[26] J. Kouvel and M. E. Fisher, Phys. Rev. A **136**, 1626 (1964).
[27] P. Butera and M. Comi, Phys. Rev. B **65**,144431 (2002).
[28] A. M. Ferrenberg and D. P. Landau, Phys. Rev. B **41**, 5081 (1991).
[29] M. Weigel and W. Janke, Phys. Rev. Lett. **102**, 100601 (2009)
[30] R. R. P. Singh and S. Chakravarty, Phys. Rev. Lett. **57**, 245 (1986).
[31] L. Klein, J. Adler, A. Aharony, A. B. Harris, Y. Meir, Phys. Rev. B **43**, 11249 (1991).
[32] D. Daboul, I. Chang and A. Aharony, Eur. Phys. J. B **41**, 231 (2004).
[33] P. H. Lundow and I. A. Campbell, Phys. Rev. B **82**, 024414 (2010).
[34] P. H. Lundow and I. A. Campbell, Phys. Rev. E **87**, 022102 (2013).

[35] P. H. Lundow and I. A. Campbell, arXiv:1210.3995.
[36] P. H. Lundow and I. A. Campbell, arXiv:1302.1100.
[37] P. H. Lundow and I. A. Campbell, arXiv:1307.5247.
[38] G. Parisi, F. Ricci-Tersenghi, and J. J. Ruiz-Lorenzo, J. Phys. A **29**, 7943 (1996).
[39] M. Ney-Nifle, Phys. Rev. B **57**, 492 (1998).
[40] The Gaussian series was calculated to 13 terms but explicit evaluation shows that there is a numerical error in the final term.
[41] E. Marinari and F. Zuliani, J. Phys. A: Math. Gen. **32**, 7447 (1999).
[42] K. Hukushima, Phys. Rev. E **60**, 3606 (1999).
[43] K. Hukushima, private communication.